

# Supplementary Information for: A multicomponent model for the prediction of nuclear waste / rare-earth extraction processes

Mario Spadina,<sup>\*,†</sup> Klemen Bohinc,<sup>‡</sup> Thomas Zemb,<sup>\*,¶</sup> and Jean-François  
Dufrêche<sup>\*,†</sup>

<sup>†</sup>*CEA, ICSM, Universite de Montpellier, 30207 Bagnols sur Ceze Cedex, France*

<sup>‡</sup>*Faculty of Health Sciences, University of Ljubljana, 1000 Ljubljana, Slovenia*

<sup>¶</sup>*CEA, ICSM, 30207 Bagnols sur Ceze Cedex, France*

E-mail: mario.spadina@cea.fr; thomas.zemb@icsm.fr; jean-francois.dufreche@icsm.fr

## Study of harmonic approximation $(p - p_0)^2$

Influence of the spontaneous packing parameter  $p_0$  on the position of the valley of zero-chain energy

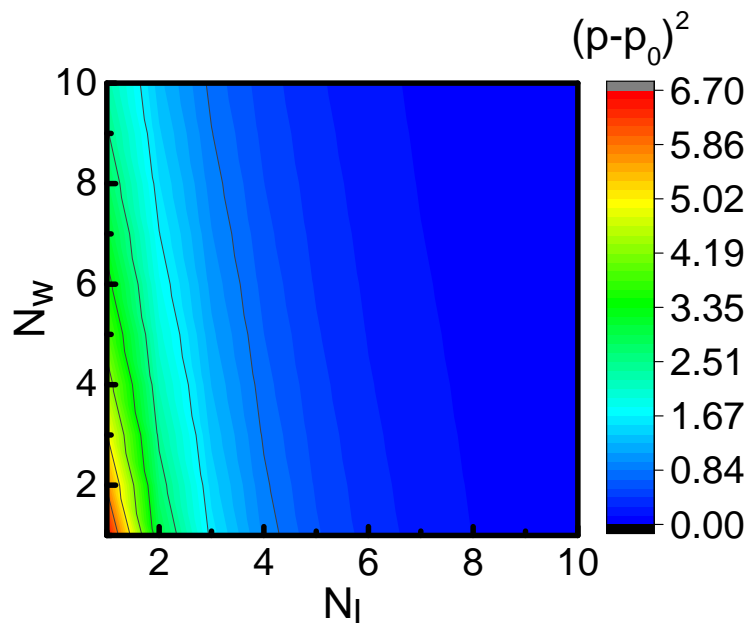


Figure S1: Map of squared differences between calculated packing parameter  $p$  for a given composition of the core of the aggregate and spontaneous packing parameter  $p_0$ . The core contains one salt molecule, namely  $\text{Eu}(\text{NO}_3)_3$ .  $N_1$  depicts number of extractant, whereas  $N_w$  depicts number of water molecules present in the core. The calculation has been made with  $p_0 = 2.5$ .

Figures S1 and S2 show a map of  $(p - p_0)^2$  as a function of composition of aggregate core. In both examples the position of the 'valley' of low  $F_{\text{chain}}$  corresponds to the high aggregation numbers and high water content.

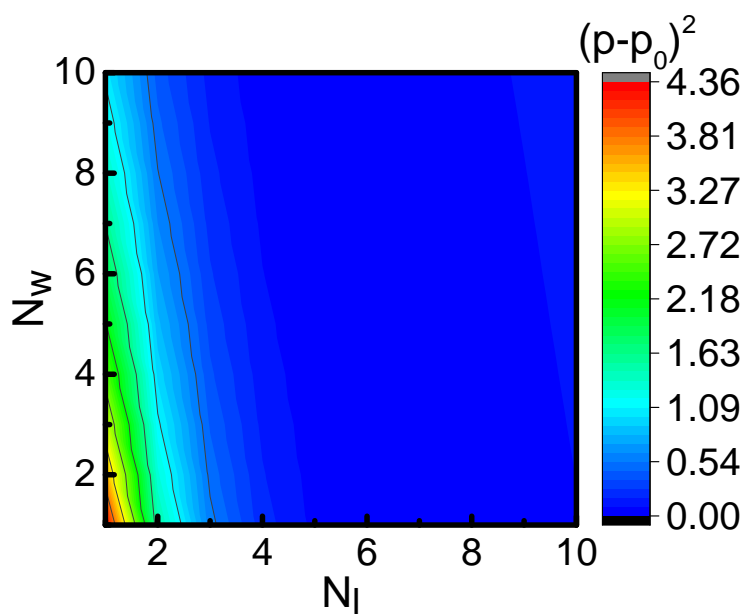


Figure S2: The map of squared differences between calculated packing parameter  $p$  and spontaneous packing parameter  $p_0$  on a composition of the core of the aggregate. The core contains one salt molecule, namely  $\text{Eu}(\text{NO}_3)_3$ .  $N_l$  depicts number of extractant, whereas  $N_w$  depicts number of water molecules present in the core. The calculation has been made with  $p_0 = 3$ .

## **Influence of spontaneous packing parameter $p_0$ on aggregate probabilities**

The value of  $p_0$  effects the equilibrium aggregate compositions. Figure S3 and S4 show the calculated probabilities of aggregates using  $p_0 = 2.5$  and 3, respectively. In both cases the method is not self-consistent, which means that the upper limit of  $N_1$  and  $N_w$  effects the results of the calculations. The most probable aggregates calculated using  $p_0 = 2.5$  and 3 do not represent a realistic picture of the aggregates (when comparing these results with experiments).

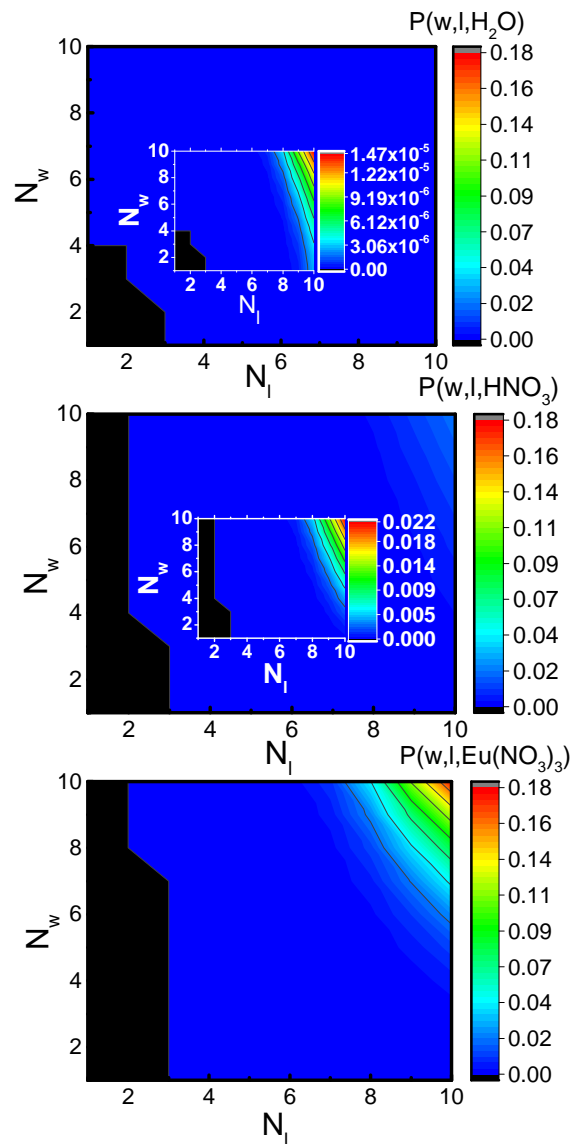


Figure S3: Calculated equilibrium aggregate probabilities as a function of the composition of the core of the aggregate.  $N_l$  depicts number of extractant, whereas  $N_w$  depicts number of water molecules present in the core. The model parameters are:  $p_0 = 2.5$ ,  $\kappa^* = 16 k_b T$  per extractant molecule,  $\mu_1^\circ = 2.5$  kJ/mol,  $E_{0,\text{HNO}_3} = 5$ ,  $E_{0,\text{Eu}(\text{NO}_3)_3} = 15.6 k_b T$  per complexed ion. System in study:  $c_{l,\text{initial}} = 0.6$  mol dm<sup>-3</sup>,  $m_{\text{H}(\text{NO}_3),\text{initial}} = 3$  mol kg<sup>-1</sup>,  $m_{\text{Eu}(\text{NO}_3)_3,\text{initial}} = 0.05$  mol kg<sup>-1</sup>. Figures show respectively the equilibrium aggregate probabilities for H<sub>2</sub>O, HNO<sub>3</sub> and Eu(NO<sub>3</sub>)<sub>3</sub> (solutes inside the core, from top to bottom). Insets in figures show scaled probabilities with purpose of easier understanding for the reader.

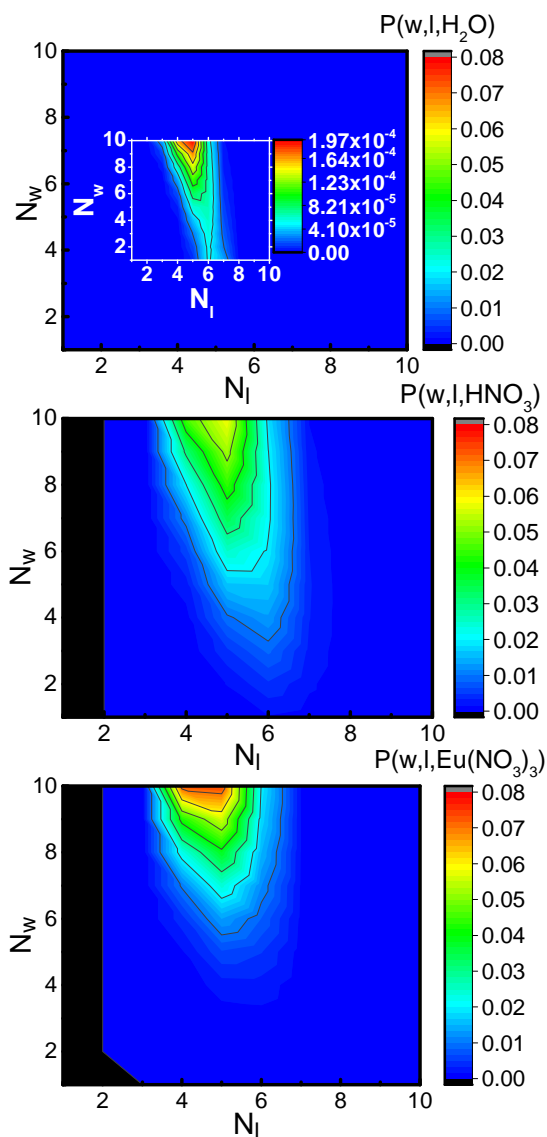


Figure S4: Dependence of the equilibrium aggregate probabilities on composition of the core of the aggregate.  $N_l$  depicts number of extractant, whereas  $N_w$  depicts number of water molecules present in the core. The model parameters are:  $p_0 = 3$ ,  $\kappa^* = 16 k_b T$  per extractant molecule,  $\mu_l^\circ = 3 \text{ kJ/mol}$ ,  $E_{0,\text{HNO}_3} = 5$ ,  $E_{0,\text{Eu}(\text{NO}_3)_3} = 15.6 k_b T$  per complexed ion. System in study:  $c_{l,\text{initial}} = 0.6 \text{ mol dm}^{-3}$ ,  $m_{\text{H}(\text{NO}_3),\text{initial}} = 3 \text{ mol kg}^{-1}$ ,  $m_{\text{Eu}(\text{NO}_3)_3,\text{initial}} = 0.05 \text{ mol kg}^{-1}$ . Figures show respectively the equilibrium aggregate probabilities for  $\text{H}_2\text{O}$ ,  $\text{HNO}_3$  and  $\text{Eu}(\text{NO}_3)_3$  (solutes inside the core, from top to bottom). Insets in figures show scaled probabilities with purpose of easier understanding for the reader.

# Influence of rigidity constant $\kappa^*$ on the chain free energy, $F_{\text{chain}}$ and aggregate probabilities

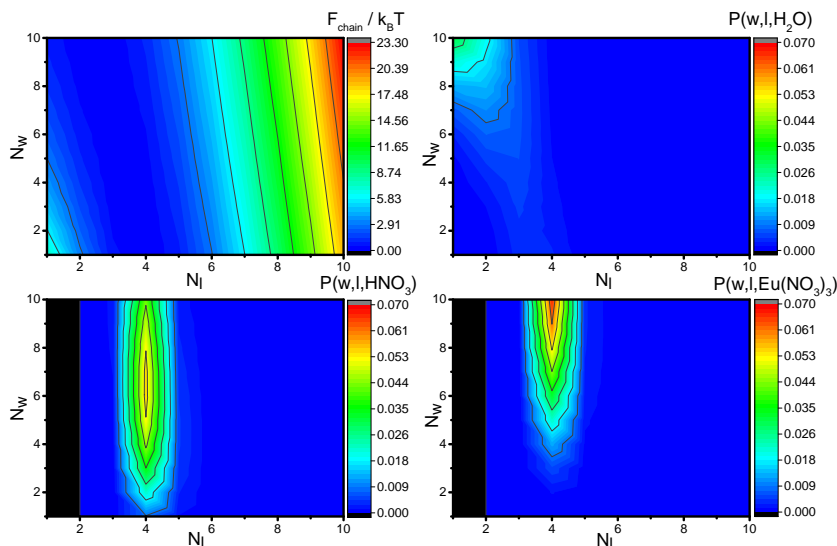


Figure S5: Dependence of the equilibrium aggregate probabilities and chain term energy on composition of the core of the aggregate. The model parameters are:  $p_0 = 3.5$ ,  $\mu_1^\circ = 3 \text{ kJ/mol}$ ,  $E_{0,\text{HNO}_3} = 5$ ,  $E_{0,\text{Eu}(\text{NO}_3)_3} = 15.6 k_B T$  per complexed ion,  $\kappa^* = 6 k_B T$  per extractant molecule. System in study:  $c_{1,\text{initial}} = 0.6 \text{ mol dm}^{-3}$ ,  $m_{\text{H}(\text{NO}_3),\text{initial}} = 3 \text{ mol kg}^{-1}$ ,  $m_{\text{Eu}(\text{NO}_3)_3,\text{initial}} = 0.05 \text{ mol kg}^{-1}$ . The upper right and the two bottom figures show respectively the equilibrium aggregate probabilities for  $\text{H}_2\text{O}$ ,  $\text{HNO}_3$  and  $\text{Eu}(\text{NO}_3)_3$  (solutes inside the core). Insets in figures show scaled probabilities with purpose of easier understanding for the reader. Results:  $\text{CAC}=0.06\text{M}$ ,  $D_{\text{Eu}^{3+}} = 14.67$

$\kappa^*$  influences the width of the chain energy valley in a way that increase of  $\kappa^*$  increases the gradient of  $F_{\text{chain}}$  plane. Consequently, higher values of  $\kappa^*$  (in our calculation  $26 k_B T$  per extractant molecule, Figure S7) allow assembly of aggregates with smaller number of water molecules. For  $\kappa^* = 6 k_B T$  the valley of low  $F_{\text{chain}}$  is rather wide so the dilution of the core of the aggregate is highly favorable. As a consequence, the unrealistic aggregates are favored.

It can be concluded that higher rigidity reduces polydispersity in terms of water content.

Distribution coefficient of  $\text{Eu}^{3+}$ ,  $D_{\text{Eu}^{3+}}$  is around 15 and CAC around 0.06 M when  $\kappa^* = 6 k_B T$ , whereas for  $\kappa^* = 26 k_B T$   $D_{\text{Eu}^{3+}}$  is around 6 and CAC around 0.08 M. The best values are obtained when  $\kappa^* = 16 k_B T$ . The extraction reads  $D_{\text{Eu}^{3+}} = 9.15$  at  $c_{1,\text{initial}} = 0.6 \text{ mol dm}^{-3}$ ,  $m_{\text{H}(\text{NO}_3),\text{initial}} = 3 \text{ mol kg}^{-1}$ ,  $m_{\text{Eu}(\text{NO}_3)_3,\text{initial}} = 0.05 \text{ mol kg}^{-1}$ .

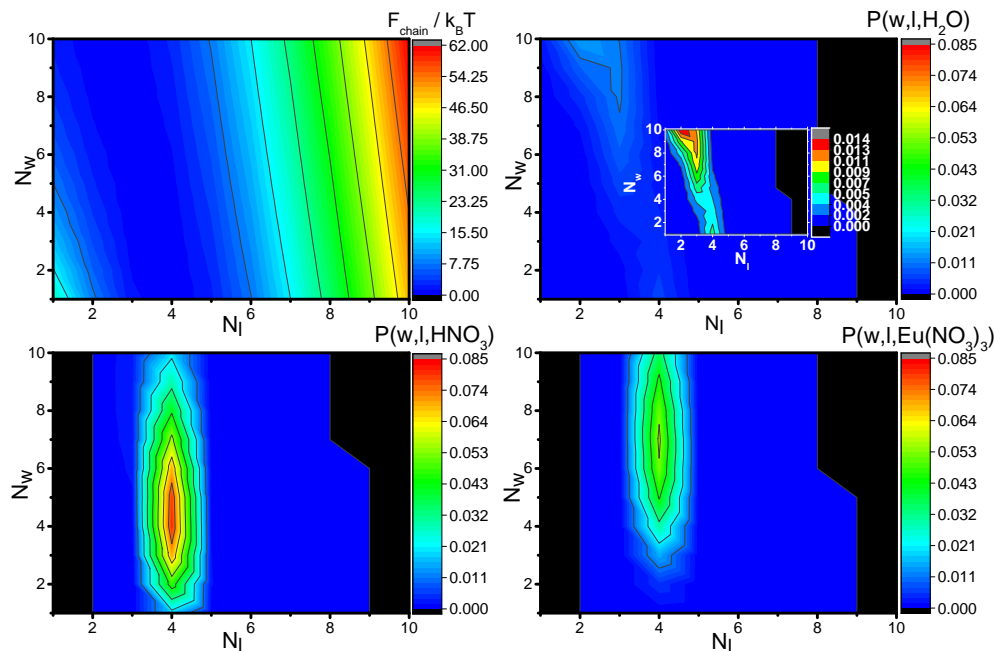


Figure S6: Dependence of the equilibrium aggregate probabilities and chain term energy on composition of the core of the aggregate. The model parameters are:  $p_0 = 3.5$ ,  $\mu_1^\circ = 3 \text{ kJ/mol}$ ,  $E_{0,\text{HNO}_3} = 5$ ,  $E_{0,\text{Eu}(\text{NO}_3)_3} = 15.6 k_B T$  per complexed ion,  $\kappa^* = 16 k_B T$  per extractant molecule. System in study:  $c_{1,\text{initial}} = 0.6 \text{ mol dm}^{-3}$ ,  $m_{\text{H}(\text{NO}_3),\text{initial}} = 3 \text{ mol kg}^{-1}$ ,  $m_{\text{Eu}(\text{NO}_3)_3,\text{initial}} = 0.05 \text{ mol kg}^{-1}$ . The upper right and the two bottom figures show respectively the equilibrium aggregate probabilities for  $\text{H}_2\text{O}$ ,  $\text{HNO}_3$  and  $\text{Eu}(\text{NO}_3)_3$  (solutes inside the core). Insets in figures show scaled probabilities with purpose of easier understanding for the reader. Results:  $\text{CAC}=0.07\text{M}$ ,  $D_{\text{Eu}^{3+}} = 9.15$



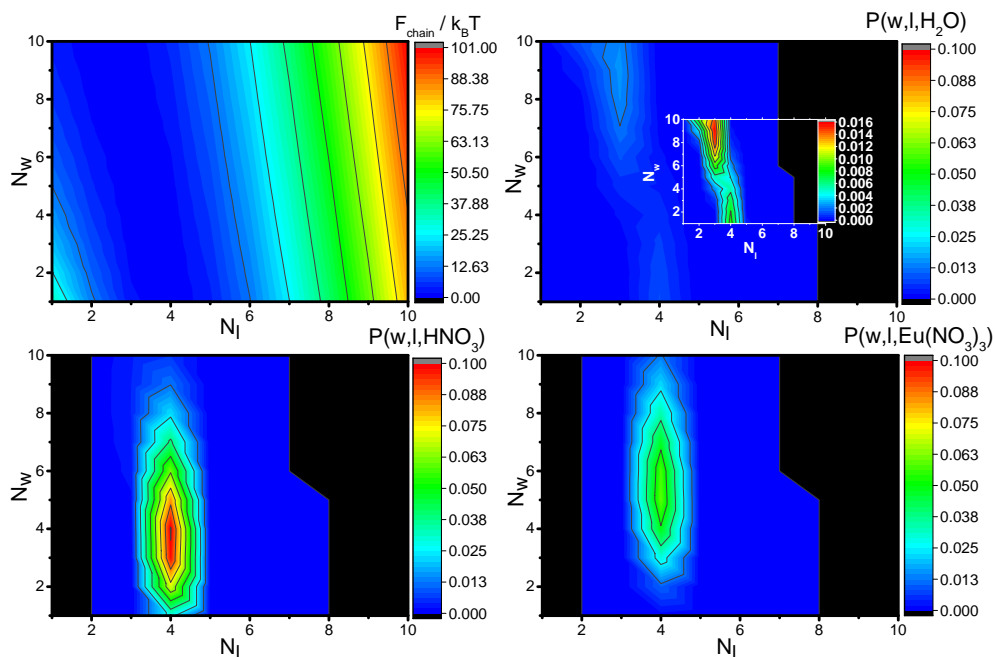


Figure S7: Dependence of the equilibrium aggregate probabilities and chain term energy on composition of the core of the aggregate. The model parameters are:  $p_0 = 3.5$ ,  $\mu_1^\circ = 3$  kJ/mol,  $E_{0,\text{HNO}_3} = 5$ ,  $E_{0,\text{Eu}(\text{NO}_3)_3} = 15.6 k_b T$  per complexed ion,  $\kappa^* = 26 k_b T$  per extractant molecule. System in study:  $c_{1,\text{initial}} = 0.6$  mol dm<sup>-3</sup>,  $m_{\text{H}(\text{NO}_3)_3,\text{initial}} = 3$  mol kg<sup>-1</sup>,  $m_{\text{Eu}(\text{NO}_3)_3,\text{initial}} = 0.05$  mol kg<sup>-1</sup>. The upper left figure shows  $F_{\text{chain}}$  as a function of the composition of aggregate core. The upper right and the two bottom figures show respectively the equilibrium aggregate probabilities for H<sub>2</sub>O, HNO<sub>3</sub> and Eu(NO<sub>3</sub>)<sub>3</sub> (solutes inside the core). Insets in figures show scaled probabilities with purpose of easier understanding for the reader. Results: CAC=0.08M,  $D_{\text{Eu}^{3+}} = 5.72$

## Aggregate probabilities at different system compositions

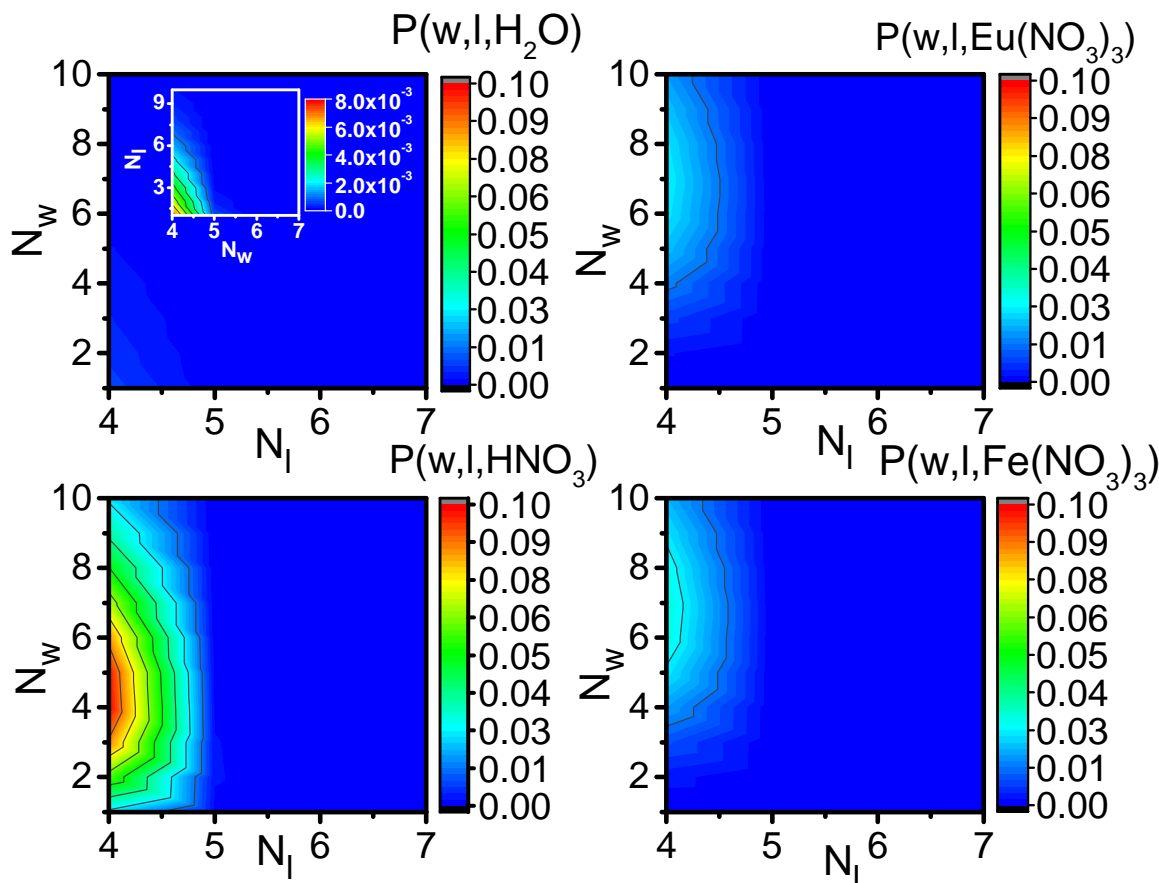


Figure S8: Dependence of the equilibrium aggregate probabilities on composition of the core of the aggregate.  $N_l$  depicts number of extractant, whereas  $N_w$  depicts number of water molecules present in the core. Scaled results of the upper left figure are shown in its inset. The model parameters are:  $p_0 = 3.5$ ,  $\kappa^* = 16 k_B T$  per extractant molecule,  $\mu_l^\circ = 2.5$  kJ/mol,  $E_{0, \text{HNO}_3} = 5 k_B T$ ,  $E_{0, \text{Fe}(\text{NO}_3)_3} = 13 k_B T$ ,  $E_{0, \text{Eu}(\text{NO}_3)_3} = 15.6 k_B T$  per complexed ion. The system in study is as follows:  $c_{l, \text{initial}} = 0.605 \text{ mol dm}^{-3}$ ,  $m_{\text{HNO}_3, \text{initial}} = 3 \text{ mol kg}^{-1}$  and  $m_{\text{Eu}(\text{NO}_3)_3, \text{initial}} = 0.02 \text{ mol kg}^{-1}$ ,  $m_{\text{Fe}(\text{NO}_3)_3, \text{initial}} = 0.05 \text{ mol kg}^{-1}$ .

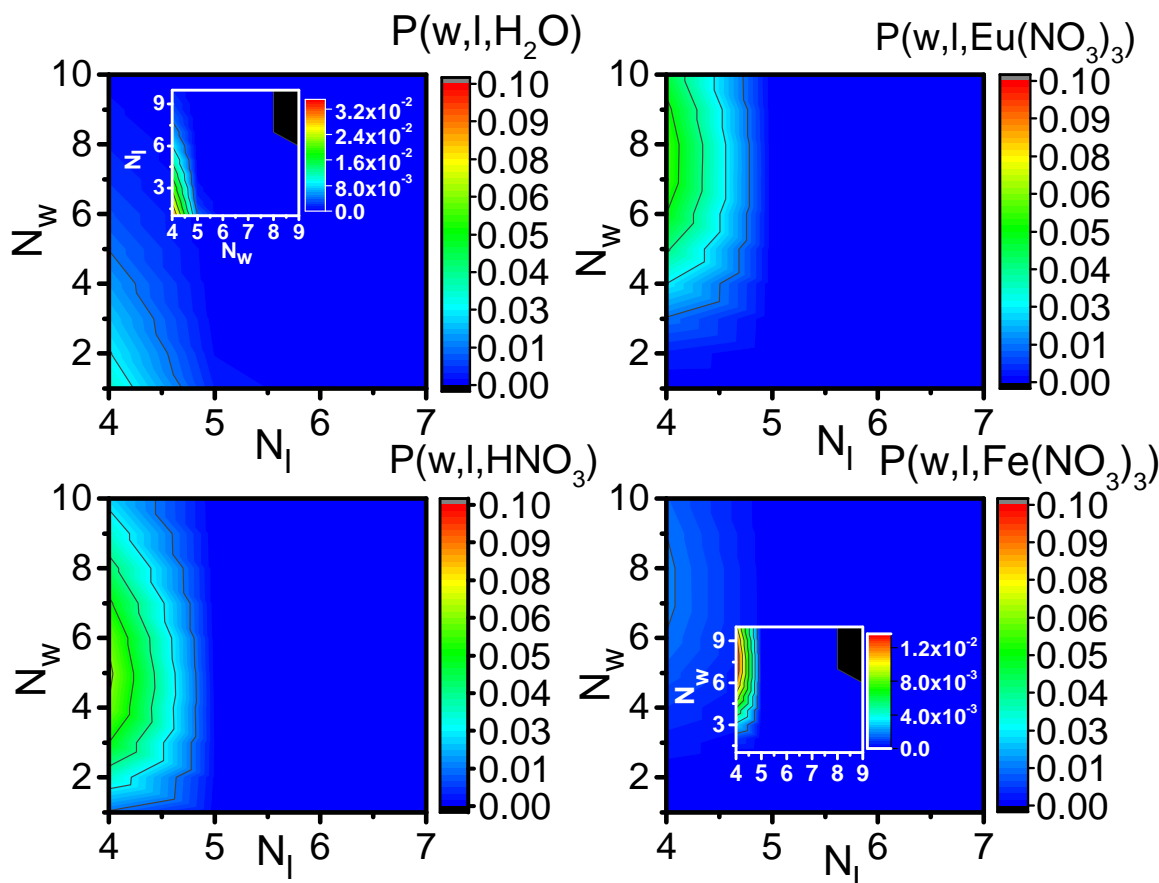


Figure S9: Dependence of the equilibrium aggregate probabilities on composition of the core of the aggregate.  $N_l$  depicts number of extractant, whereas  $N_w$  depicts number of water molecules present in the core. Scaled results of the upper left and lower right figure are shown in its insets. The model parameters are:  $p_0 = 3.5$ ,  $\kappa^* = 16 k_B T$  per extractant molecule,  $\mu_1^\circ = 2.5$  kJ/mol,  $E_{0,HNO_3} = 5 k_B T$ ,  $E_{0,Fe(NO_3)_3} = 13 k_B T$ ,  $E_{0,Eu(NO_3)_3} = 15.6 k_B T$  per complexed ion. The system in study is as follows:  $c_{l,initial} = 0.605$  mol dm $^{-3}$ ,  $m_{HNO_3,initial} = 1$  mol kg $^{-1}$  and  $m_{Eu(NO_3)_3,initial} = 0.05$  mol kg $^{-1}$ ,  $m_{Fe(NO_3)_3,initial} = 0.05$  mol kg $^{-1}$ .

## The extraction of metal ions at various physical conditions

The extraction curve presented in Figure S12 shows the influence of  $c_{1,\text{initial}}$  on  $D_{\text{Eu}^{3+}}$ . The results are shown for various  $\text{HNO}_3$  concentration, ranging from 0.5 to 5 mol kg<sup>-1</sup>.

The results show the nonlinear increase of distribution coefficients with increasing  $c_{1,\text{initial}}$ . The increase in  $m_{\text{HNO}_3,\text{initial}}$  causes an increase in  $D_{\text{Cat},i}$  which means that the extraction is enhanced upon addition of  $\text{HNO}_3$  the system. This is a consequence of the decrease of gradient of  $\text{NO}_3^-$  concentrations between aqueous phase and the concentration in the core of aggregates.

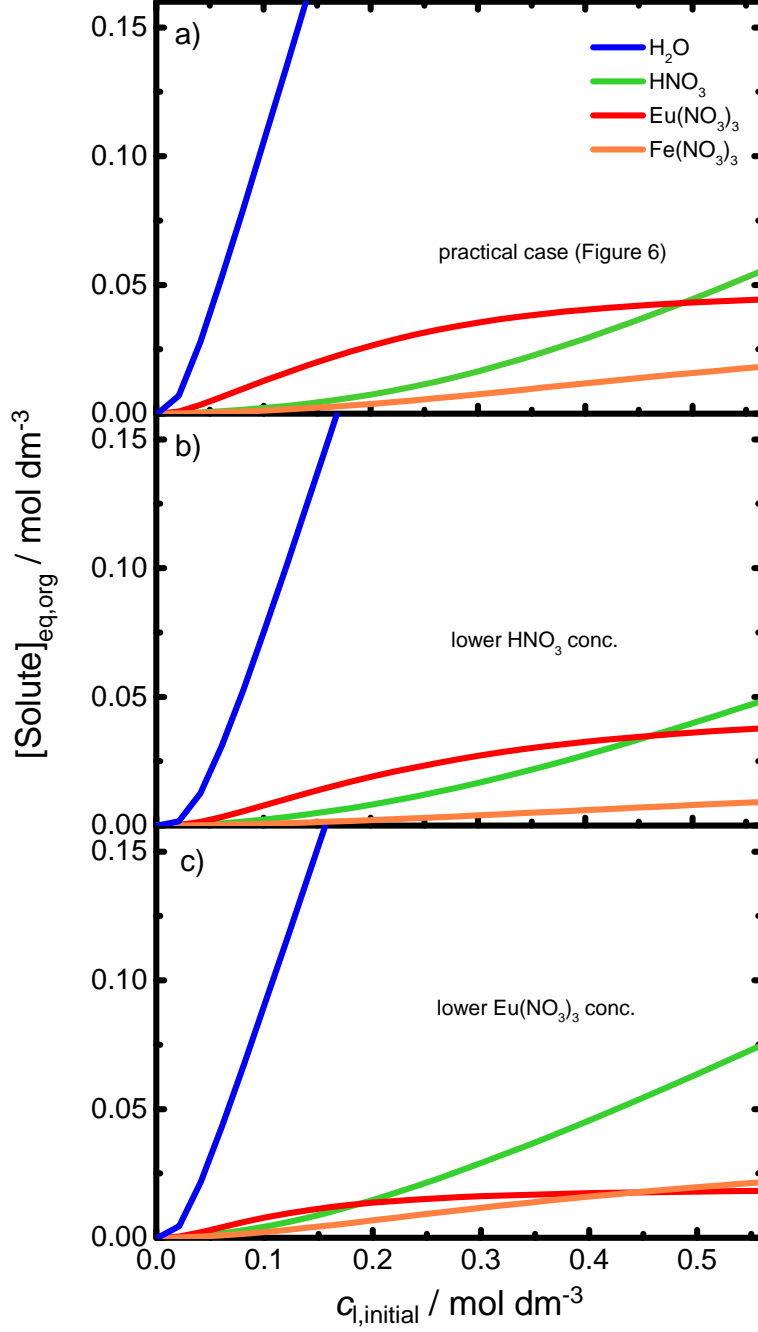


Figure S10: Calculated equilibrium concentrations of all extracted solutes as a function of the initial extractant concentration. The model parameters are:  $p_0 = 3.5$ ,  $\kappa^* = 16 k_B T$  per extractant molecule,  $\mu_1^0 = 2.5 \text{ kJ/mol}$ ,  $E_{0,\text{HNO}_3} = 5 k_B T$ ,  $E_{0,\text{Fe}(\text{NO}_3)_3} = 13 k_B T$ ,  $E_{0,\text{Eu}(\text{NO}_3)_3} = 15.6 k_B T$  per complexed ion. a)  $m_{\text{HNO}_3,\text{initial}} = 3 \text{ mol kg}^{-1}$ ,  $m_{\text{Eu}(\text{NO}_3)_3,\text{initial}} = m_{\text{Fe}(\text{NO}_3)_3,\text{initial}} = 0.05 \text{ mol kg}^{-1}$ . b)  $m_{\text{HNO}_3,\text{initial}} = 1 \text{ mol kg}^{-1}$ ,  $m_{\text{Eu}(\text{NO}_3)_3,\text{initial}} = m_{\text{Fe}(\text{NO}_3)_3,\text{initial}} = 0.05 \text{ mol kg}^{-1}$ . c)  $m_{\text{HNO}_3,\text{initial}} = 3 \text{ mol kg}^{-1}$ ,  $m_{\text{Eu}(\text{NO}_3)_3,\text{initial}} = 0.02 \text{ mol kg}^{-1}$ ,  $m_{\text{Fe}(\text{NO}_3)_3,\text{initial}} = 0.05 \text{ mol kg}^{-1}$ .

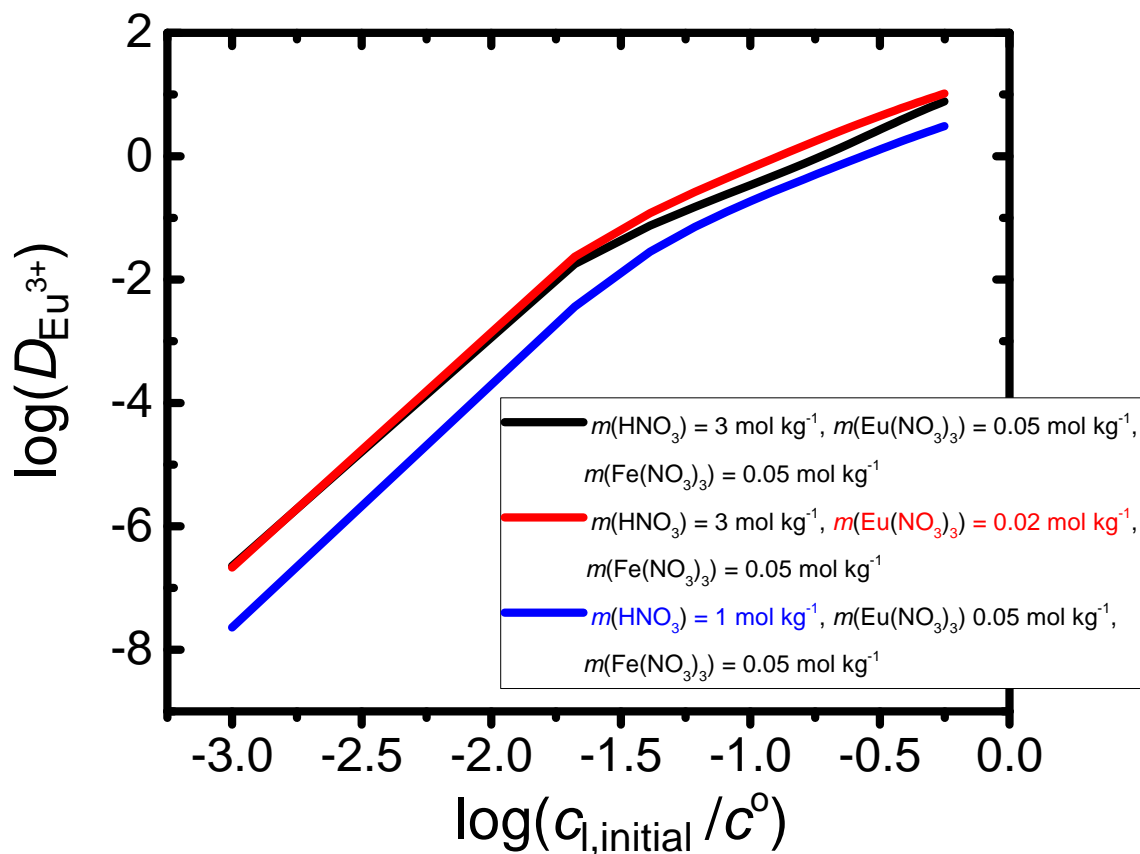


Figure S11: Decimal logarithm of  $\text{Eu}^{3+}$  distribution coefficient as a function of decimal logarithm of the initial extractant concentration. The model parameters are:  $p_0 = 3.5$ ,  $\kappa^* = 16 k_B T$  per extractant molecule,  $\mu_1^\circ = 2.5 \text{ kJ/mol}$ ,  $E_{0,\text{HNO}_3} = 5 k_B T$ ,  $E_{0,\text{Fe}(\text{NO}_3)_3} = 13 k_B T$ ,  $E_{0,\text{Eu}(\text{NO}_3)_3} = 15.6 k_B T$  per complexed ion. The black curve depicts the system:  $m_{\text{HNO}_3,\text{initial}} = 3 \text{ mol kg}^{-1}$ ,  $m_{\text{Eu}(\text{NO}_3)_3,\text{initial}} = m_{\text{Fe}(\text{NO}_3)_3,\text{initial}} = 0.05 \text{ mol kg}^{-1}$ . The red curve depicts the system:  $m_{\text{HNO}_3,\text{initial}} = 3 \text{ mol kg}^{-1}$ ,  $m_{\text{Eu}(\text{NO}_3)_3,\text{initial}} = 0.02 \text{ mol kg}^{-1}$ ,  $m_{\text{Fe}(\text{NO}_3)_3,\text{initial}} = 0.05 \text{ mol kg}^{-1}$ . The blue curve depicts the system:  $m_{\text{HNO}_3,\text{initial}} = 1 \text{ mol kg}^{-1}$ ,  $m_{\text{Eu}(\text{NO}_3)_3,\text{initial}} = m_{\text{Fe}(\text{NO}_3)_3,\text{initial}} = 0.05 \text{ mol kg}^{-1}$ .

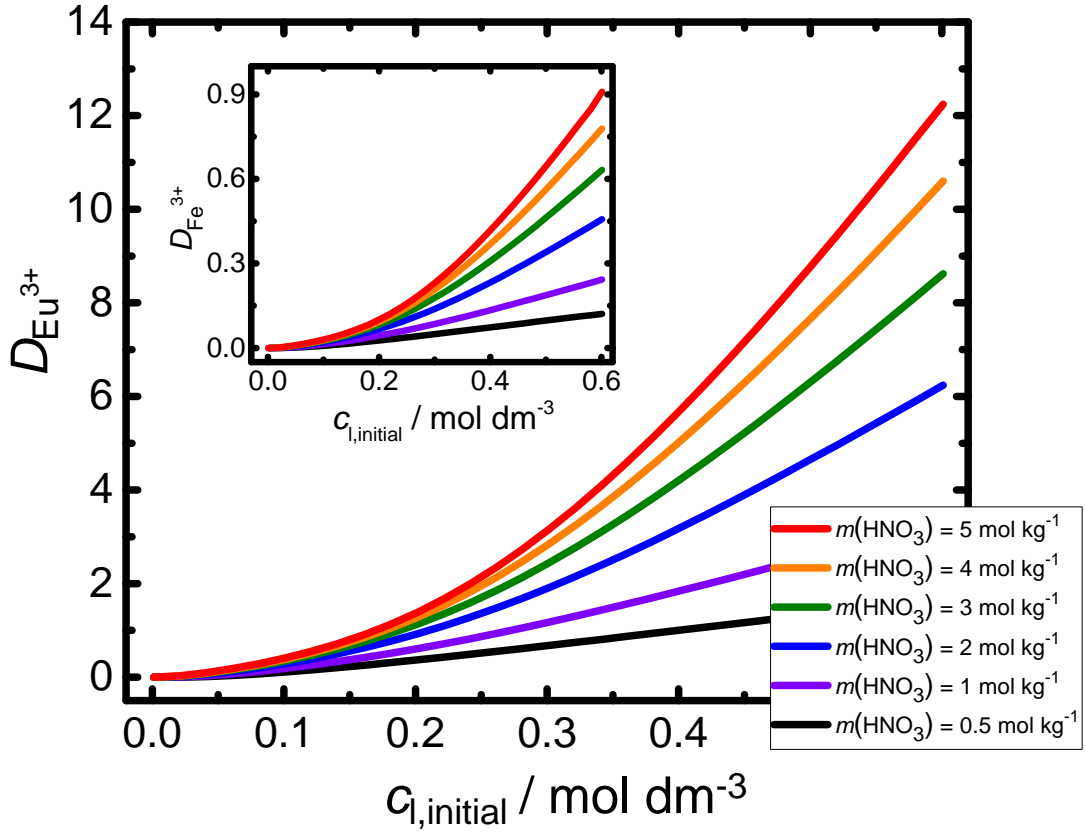


Figure S12:  $D_{\text{Eu}^{3+}}$  as a function of the initial extractant concentration. The model parameters are:  $p_0 = 3.5$ ,  $\kappa^* = 16 k_B T$  per extractant molecule,  $\mu_1^\circ = 2.5 \text{ kJ/mol}$ ,  $E_{0,\text{HNO}_3} = 5 k_B T$ ,  $E_{0,\text{Fe}(\text{NO}_3)_3} = 13 k_B T$ ,  $E_{0,\text{Eu}(\text{NO}_3)_3} = 15.6 k_B T$  per complexed ion. The system in study is:  $m_{\text{Eu}(\text{NO}_3)_3,\text{initial}} = m_{\text{Fe}(\text{NO}_3)_3,\text{initial}} = 0.05 \text{ mol kg}^{-1}$ . The results are presented for various concentrations of nitric acid in aqueous phase. The equivalent curve for the extraction of  $\text{Fe}^{3+}$  is presented in the inset.